



# Choroidal Neovascularization Associated with Best Vitelliform Macular Dystrophy

 Seda Karaca Adiyeye,  Gamze Ture

Department of Ophthalmology, Tepecik Research and Training Hospital, Izmir, Turkey

## Abstract

**Objectives:** The aim of the study was to evaluate the clinical and optical coherence tomography (OCT) findings of patients with choroidal neovascularization (CNV) due to best vitelliform macular dystrophy (BVMD).

**Methods:** Six eyes that were diagnosed with CNV associated with BVMD were evaluated retrospectively. A standard ophthalmologic examination, a fundus fluorescein angiography (FA), and the OCT findings of the patients were examined. Anatomical and functional changes seen after treatment were evaluated.

**Results:** One (16%) of the cases was female and five (83%) were male. The mean age was calculated as  $36.3 \pm 24.9$  years (range 11–73 years). The mean follow-up period of the cases after detecting CNV was determined as 26 months (range 6–168 months). Best corrected visual acuities were  $0.65 \pm 0.39$  logMAR (1.0–0.2 logMAR) when CNV was detected and  $0.42 \pm 0.25$  logMAR (limits 0.7–0.2 logMAR) at the end of the follow-up. Photodynamic therapy was applied to one (17%) of the cases, and intravitreal anti-vascular endothelial growth factor (anti-VEGF) treatment was applied to the others (83%). The mean number of intravitreal injections was found to be  $3 \pm 1.37$  (range 2–4).

In all cases, intraretinal fluid (IRF), subretinal fluid (SRF), external limiting membrane, and irregularities in inner retinal layers were observed in the initial OCT examinations. In all cases, it was observed that the IRF regressed with treatment and SRF continued in five eyes. Hypertrophic outer retinal scarring developed in all cases.

**Conclusion:** In cases with CNV due to BVMD, regression in CNV activity was achieved with intravitreal anti-VEGF injection treatment. The IRF is a marker that can be used both in the diagnosis and treatment monitoring of CNV associated with BVMD.

**Keywords:** Best vitelliform macular dystrophy, choroidal neovascularization, optic coherence tomography

## Introduction

Best vitelliform macular dystrophy (BVMD) is a disease caused by an inherited autosomal dominant mutation of the gene encoding the bestrophin protein, an ion channel protein, in the retinal pigment epithelium (1,2). It is characterized by the bilateral accumulation of subretinal yellow material with a later eruption into the photoreceptor layer and a symptomatic reduction in vision (3).

Five different stages of the disease have been identified: Previtelliform, vitelliform, pseudohypopyon, vitelliruptive, and atrophic cicatricial (4). The most serious complication of the disease is choroidal neovascularization (CNV), which is seen in 20%. CNV occurs as a late complication as a result of damage to retina pigment epithelium (RPE) and the Bruch membrane (5). In the treatment of CNV secondary to BVMD, laser photocoagulation, untreated observation, (6)

**How to cite this article:** Karaca Adiyeye S, Ture G. Choroidal Neovascularization Associated with Best Vitelliform Macular Dystrophy. *Beyoglu Eye J* 2022; 7(2): 103-108.

**Address for correspondence:** Seda Karaca Adiyeye, MD. Goz Hastaliklari Anabilim Dali,  
Tepecik Egitim ve Arastirma Hastanesi, Izmir, Turkey

**Phone:** +90 532 610 26 21 **E-mail:** skaracaadiyeye@hotmail.com

**Submitted Date:** January 29, 2021 **Accepted Date:** March 14, 2022 **Available Online Date:** May 27, 2022

©Copyright 2022 by Beyoglu Eye Training and Research Hospital - Available online at [www.beyoglueye.com](http://www.beyoglueye.com)

OPEN ACCESS This work is licensed under a Creative Commons Attribution-NonCommercial-ShareAlike 4.0 International License.



photodynamic therapy, (7) laser photocoagulation, and intravitreal anti-vascular endothelial growth factor (VEGF) are applied (8,9).

Optical coherence tomography (OCT) is important in the diagnosis and follow-up of BVMD as a non-invasive technique in identifying vitelliform material and evaluating subretinal fluid (SRF) and retinal layers (10). In our study, we aimed to evaluate the clinical findings, OCT findings, and response to the treatment of cases with BVMD-associated CNV development.

## Methods

All cases followed up with the diagnosis of BVMD between September 2006 and December 2020 were analyzed. The data of patients with CNV were evaluated retrospectively. The study was conducted in accordance with the Helsinki Criteria and was approved by the Local Ethics Committee. (2020/14-64).

Detailed medical histories and demographic data, such as age and gender of participants, were recorded. The best corrected visual acuities (BCVA) of the subjects were measured with the Snellen chart and converted to the logarithm of the minimum resolution angle equivalent (logMAR) for statistical analysis. Anterior segment and fundus examination findings, OCT, and fluorescein angiography (FA) data of all cases were evaluated.

Color fundus photographs and FA images were taken with Topcon TRC-50IX (Topcon, Tokyo, Japan) and ZEISS VISUCAM 500 (Carl Zeiss Meditec, Jena, Germany) fundus cameras; spectral domain (SD)-OCT images were obtained using Spectralis OCT (Heidelberg Engineering, Heidelberg, Germany). Acute visual deterioration, retinal hemorrhage on fundus examination, leakage compatible with CNV in FA examination, detection of intraretinal fluid (IRF) and irregular retinal pigment epithelium detachment in OCT were evaluated to be compatible with active CNV. Continuity of the retinal layers, RPE elevation, and the presence of IRF and SRF in the OCT examination were also examined.

## Statistical Analysis

Statistical analysis of the data was performed using the SPSS 20.0 (IBM Corp., Armonk, NY, USA) statistical package program. Statistical data were expressed as mean±standard deviations (mean±SD). Descriptive statistics were expressed as frequency and percentage. The data were compared by the Wilcoxon signed rank test. The statistical significance level was  $p<0.05$  for all analyses.

## Results

Six eyes of six patients were included in our study. It was observed that the right eye of a patient was compatible with

active CNV, while the left eye was compatible with inactive CNV. The eye of a patient with inactive CNV was not included in the study. In all other cases, CNV was detected in one eye.

The mean age of the cases at the time of CNV was calculated as  $36.3\pm 24.9$  years (range 11–73 years). One (16%) of the cases was female and five (83%) were male. In two of the cases (33%), CNV was detected while being followed up with a diagnosis of BVMD. In four (67%) patients, secondary CNV was detected in their first admission with the complaint of decreased visual acuity.

The mean follow-up period after CNV detection of the cases was determined as 26 months (range 6–168 months). Fundus examination of one patient showed subretinal yellow material accumulation and retinal elevation in the inferior of the lesion. Atrophic retinal pigment epithelial changes and elevation were observed in other cases. Subretinal hemorrhage was observed in all cases.

FA was revealed blocking hypofluorescence resulting from a subretinal hemorrhage and early hyperfluorescence with intense late leakage, thereby confirming CNV. Except for CNV, fluorescein blockage due to material accumulation in one case (Fig. 1a-c) and hyperfluorescence due to a window defect in atrophic areas in other cases were observed in FA. CNV was located subfoveal in three cases, at the superior half of the vitelliform lesion in one case (Fig. 1a) and at the inferior half of the vitelliform lesion in two cases.

Mean BCVA was  $0.65\pm 0.39$  logMAR (1.0–0.2 logMAR) when CNV was detected. After treatment, it was determined to be  $0.42\pm 0.25$  logMAR (range 0.7–0.2 logMAR). BCVA increased in 4 patients (67%), while the BCVA of 2 patients (33%) remained at the same level. A statistically significant increase in BCVA was found with the treatment in our study ( $p=0.012$ ). Photodynamic therapy was applied to one of the cases, and intravitreal anti-VEGF therapy was applied to the other five cases. Intravitreal ranibizumab treatment (0.5 mg/0.1 ml) was administered in two patients and intravitreal bevacizumab treatment (1.25 mg/0.05 ml) in three patients. The mean number of intravitreal injection of the cases was  $3\pm 1.37$  (range 2–4).

None of the cases developed complications due to intravitreal injections. When the initial OCT examination of the cases was evaluated, all had irregular RPE elevations, IRF, and SRF. Irregularity was observed in the external limiting membrane (ELM) and inner retinal layers in the acute period (Figs. 2a-e and 3a-e). Hyperreflective dots were not observed in any of the cases.

Choroidal excavation was detected in two cases. A choroidal excavation was found in one patient when CNV was detected, while a choroidal excavation developed in the other patient during follow-up after the treatment (Fig. 4a-c).

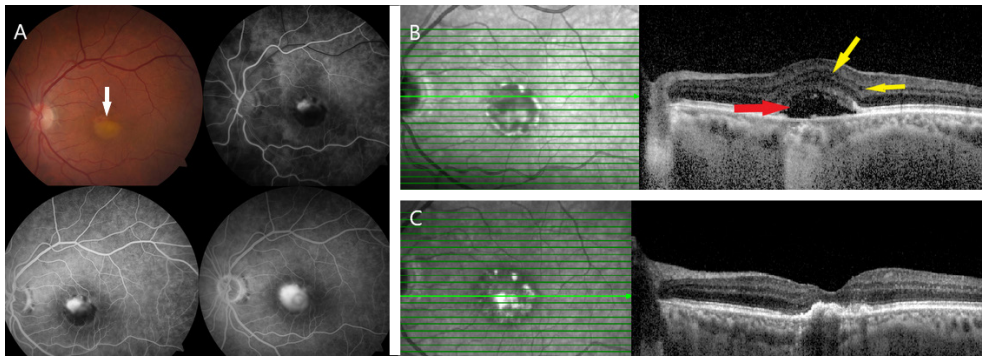


**Figure 1.** Fundus fluorescein angiography in acute phase (FA) (**a**) and optical coherence tomography (OCT) images of case number 5 (**b and c**). A streak-shaped subretinal hemorrhage (white arrow) is seen in color fundus photography. (**a**) In FA, fluorescein blockage due to material accumulation, leakage in the early period in accordance with choroidal neovascularization, and an increase in the size and density of the leak in the late period are observed (**a**). Intraretinal fluid (IRF) (yellow arrow), subretinal fluid (SRF) (red arrow), and external limiting membrane (ELM) irregularities are seen in the pre-treatment OCT examination (**b**). It is observed that ELM irregularity does not improve, SRF disappears, and hypertrophic scarring develops in the follow-up of the patient after two intravitreal bevacizumab injections (**c**).

IRF disappeared in the 1st month after the first intravitreal injection in all cases.

SRF persisted in five eyes, although CNV activation regressed after the treatment. Further, after the treatment, hypertrophic outer retinal scarring developed in all cases. In two cases, in the follow-up, while ELM was observed irregu-

larly in the active CNV period, ELM integrity was regained on the hypertrophic scar with treatment, and the retinal layers were monitored regularly (Figs. 2d-e and 3c-e). In the other four cases, the ELM and retinal layers were predominantly irregular in the scar and lesion areas. The clinical findings were summarized in Table I.

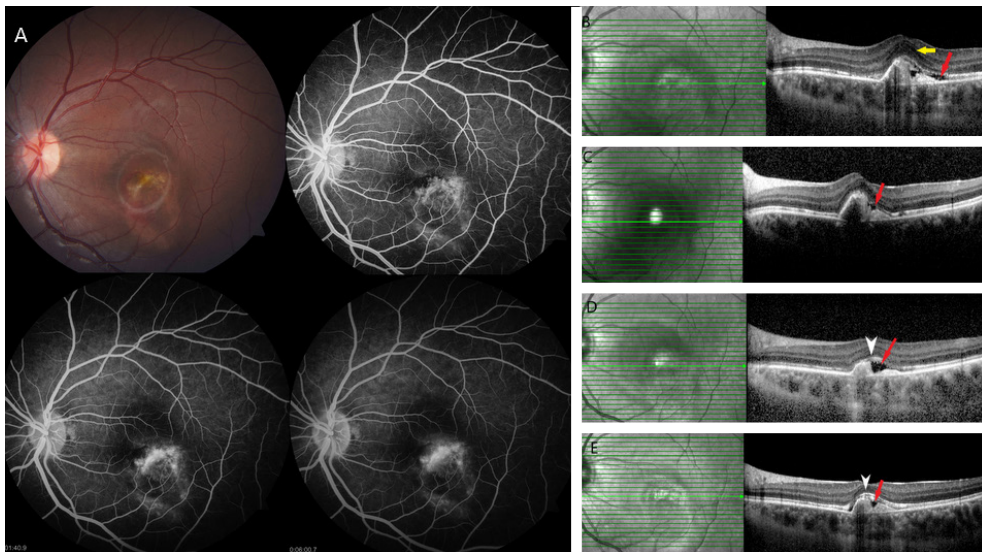


**Figure 2.** Fundus fluorescein angiography (FA) and optical coherence tomography (OCT) images of case number four. Hypofluorescence due to subretinal hemorrhage, leakage in the early period in accordance with choroidal neovascularization, and an increase in the size and density of the leak in the late period are observed in FA (**a**). Intraretinal fluid (IRF) (yellow arrow), subretinal fluid (SRF) (red arrow), and irregularity in the inner retinal layers are seen in the pre-treatment OCT examination (**b**). After the first intravitreal bevacizumab (IVB) injection, the IRF has disappeared, and the SRF continues (**c**). After the second IVB application, the inner retinal layers are regular and the ELM [(white arrowhead), (ELM)] begins to become regular (**d**). In the follow-up after the third IVB application, SRF continues, hypertrophic scarring develops, and ELM is regular (**e**).

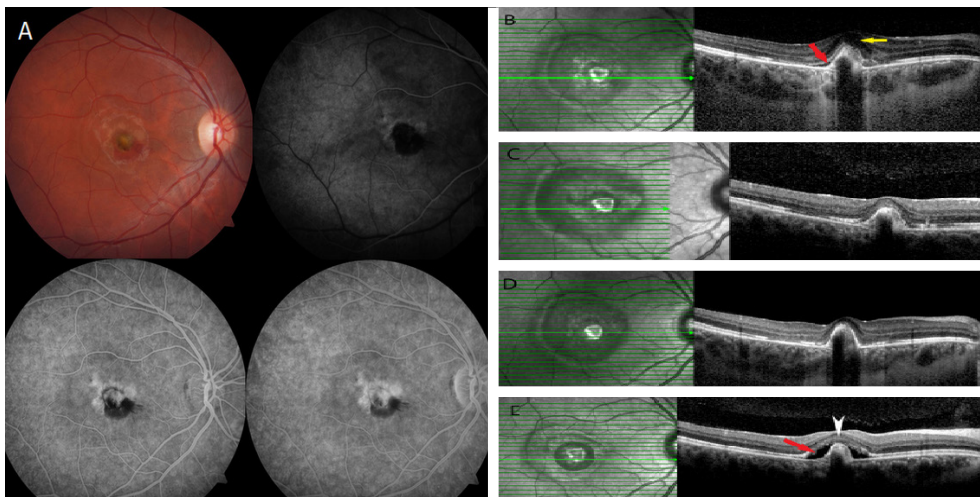


**Figure 3.** Fundus fluorescein angiography (FA) and optical coherence tomography (OCT) images of case number 6. Hypofluorescence due to subretinal hemorrhage, leakage in the early period in accordance with choroidal neovascularization, and an increase in the size and density of the leak in the late period are observed in FA (a). In pre-treatment OCT examination, intraretinal fluid (IRF) (yellow arrow) and subretinal fluid (SRF) (red arrow), and irregularity in the inner retinal layers are seen (b). IRF and SRF disappear after the first intravitreal bevacizumab (IVB) injection (c). After the second IVB injection that the inner retinal layers begin to become regular in the areas adjacent to the lesion (d). SRF continues and hypertrophic scarring develops after the third IVB application. ELM (white arrowhead) appears to be regenerated (e).

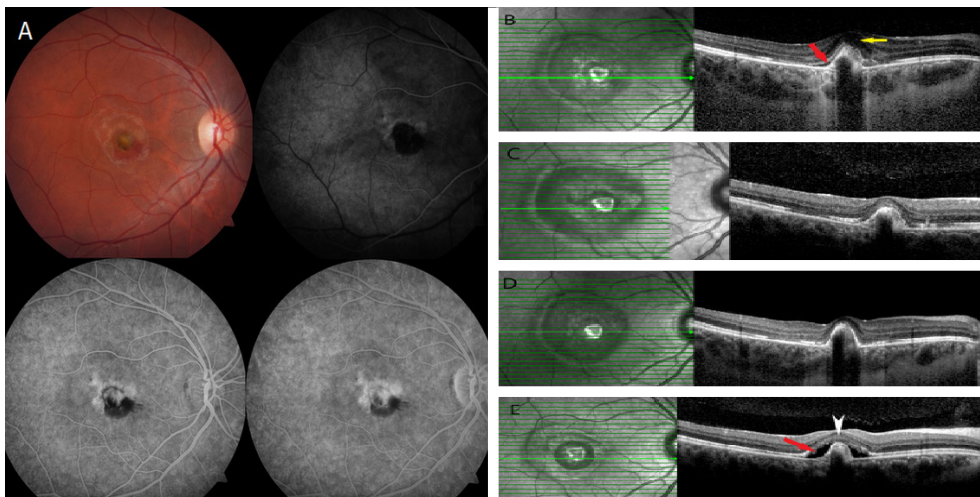


**Figure 4.** Fundus fluorescein angiography in the acute phase (FA) (a), color fundus photograph after photodynamic therapy (b), and optical coherence tomography (OCT) images (c) of case number 1. In FA, hypofluorescence due to subretinal hemorrhage, leakage in the early period in accordance with choroidal neovascularization, and increase in the size and density of the leakage in the late period are observed (a). Hypertrophic scarring and choroidal excavation are observed in the follow-up of the patient who has undergone applied photodynamic therapy (c).

## Discussion

BVMD is characterized by good vision up to the sixth decade unless complicated by choroidal neovascularization. RPE dysfunction causes fluid accumulation in the subretinal space, causing retinal layers to move away from the RPE. Thus, the phagocytosis of the photoreceptor's outer segment is re-

duced. Increased oxidative stress increases the accumulation of lipofuscin, causing an increase in free radicals and retinal damage. The severity of RPE dysfunction and the increase in oxidative stress are thought to initiate the development of BVD-induced CNV (11).

Spaide et al. stated that the accumulation of high autofluorescent material in the outer retina consists of non-digest-

**Table 1.** Clinical and optic coherence tomography findings of the patient

Patient No	Age/gender	Initial BCVA (logMAR)	Final BCVA (logMAR)	Initial OCT findings	Final OCT findings	Treatment
1	43/M	1.0	0.7	SH+IRF+SRF+	SRF+Hypertrophic scar Choroidal excavation	Photodynamic therapy
2	39/F	1.0	0.5	SH+IRF+SRF+	SRF+Hypertrophic scar Choroidal excavation	4 IVR
3	9/M	1.0	0.7	SH+IRF+SRF+	SRF+Hypertrophic scar	3 IVR
4	19/M	0.2	0.2	SH+IRF+SRF+	SRF+Hypertrophic scar	3 IVB
5	73/M	0.2	0.2	SH+IRF+SRF+	Hypertrophic scar	2 IVB
6	11/M	0.5	0.2	SH+IRF+SRF+	SRF+Hypertrophic scar	3 IVB

IVR: Intravitreal ranibizumab injection; IVB: Intravitreal Bevacizumab injection; SRF: Subretinal fluid; IRF: Intraretinal fluid; SH: subretinal hemorrhage; BCVA: Best corrected visual acuities; OCT: Optical coherence tomography.

ible phagocytosed outer segments of photoreceptors and the accumulation of lipofuscin (3).

It has been shown that in CNV cases secondary to macular dystrophies, the visual prognosis is better, and the number of intravitreal injections applied is lower compared to AMD (12). In these cases, CNV spontaneously transforms into a small fibrotic scar with no treatment (12). Despite the spontaneous involution, patients who received intravitreal anti-VEGF injection achieved better visual acuity compared to patients without the treatment (9). In our study, the treatment was applied to all cases, and a significant increase in visual acuity was found.

In many studies on CNV due to BVMD, regression in CNV activation was found with a small number of intravitreal injections (13-15). In our study, the regression of IRF after the first IV injection in all cases, and the fact that ELM continuity started to be restored in places, intermittently suggests that anti-VEGF sensitivity is high in BVMD cases.

In BVMD cases, CNV often develops in the lower half of the vitelliform lesion due to the accumulation of gravity affecting the inferior retina-RPE complex more than upper half (9). On the contrary, in our study, we found that CNV was located in the subfoveal in two cases, in the lower half of the lesion in two cases and in the upper half of the lesion in two cases. Parodi et al.(16) described the OCT findings in the BVMD stages. In these cases, they described deterioration in the RPE, the ellipsoid zone and ELM layers in all stages, although there was less deterioration in the previtelliform stage. In our study, we observed an irregularity in the outer retinal layers (ORL) and IRF accumulation during the period when active CNV was detected. We found that the first finding that resolved with anti-VEGF treatment was IRF and that ELM was restored intermittently in the lesion area during follow-up. We think that ELM and ORL irregularity cannot be considered as a marker

in the evaluation of the presence of CNV, since irregularities are detected in the ORL at all stages of the disease. Despite this, the fact that the ORL irregularity was observed at the beginning and reorganized with the treatment may be a marker in terms of evaluating the effectiveness of the treatment. IRF is rare, even in very advanced stages of the disease (9). Therefore, IRF can be useful in evaluating the diagnosis and treatment efficiency in the presence of active CNV.

Choroidal excavation was detected in two of our cases. Parodi et al. reported that choroidal excavation may develop in BVMD cases due to severe chorioretinal degeneration (16). In studies examining CNV due to BVMD, the researchers found that SRF continued despite the regression of CNV (9). In our study, we observed that SRF continued in the presence of inactive CNV. In the studies of Parodi et al., in which long-term follow-up results of BVMD cases were evaluated, it was observed that the solid vitelliform lesion transformed into a vitelliform lesion with SRF over time (17). For this reason, we think that SRF cannot be used in CNV diagnosis and follow-up treatment.

The retrospective design and the low number of cases are the limiting factors of our study. We think that prospective studies including a large number of cases in which these cases are evaluated with OCT angiography in addition to OCT will be useful. As a result, choroidal neovascularization associated with BVMD is sensitive to anti-VEGF treatments. IRF seen in OCT can be used as a marker in evaluating the presence of CNV and in response to the treatment during follow-up.

#### Disclosures

**Ethics Committee Approval:** All cases followed up with the diagnosis of BVMD between September 2006 and December 2020 were analyzed. The data of patients with CNV were evaluated retrospectively. The study was conducted in accordance with the Helsinki Criteria and was approved by the Local Ethics Committee. (2020/14-64).

**Peer-review:** Externally peer-reviewed.

**Conflict of Interest:** None declared.

**Authorship Contributions:** Concept – G.T.; Design – S.K.A.; Supervision – G.T.; Data Collection and/or Processing – S.K.A., G.T.; Analysis and/or Interpretation – S.K.A., G.T.; Literature Search – S.K.A., G.T.; Writing – S.K.A., G.T.; Critical Reviews – G.T.

## References

- Marmorstein AD, Marmorstein LY, Rayborn M, Xinxing W, Hollyfield JG, Ptukhin K. Bestrophin, the product of the Best vitelliform macular dystrophy gene (VMD2), localizes to the basolateral plasma membrane of the retinal pigment epithelium. *Proc Natl Acad Sci* 2000;97:12758–63. [\[CrossRef\]](#)
- Blodi CF, Stone EM. Best's vitelliform dystrophy. *Ophthalmic Paediatr Genet* 1990;11:49–59.
- Spaide RF, Noble K, Morgan A, Freud KB. Vitelliform macular dystrophy. *Ophthalmology* 2006;113:1392–400. [\[CrossRef\]](#)
- Gass JD. Stereoscopic atlas of macular diseases. Diagnosis and treatment. *Arch Ophthalmol* 1989;107:26. [\[CrossRef\]](#)
- Tsang SH, Sharma T. Best vitelliform macular dystrophy. *Adv Exp Med Biol* 2018;1085:79–90. [\[CrossRef\]](#)
- Viola F, Villani E, Mapelli C, Staurengi G, Ratiglia R. Bilateral juvenile choroidal neovascularization associated with Best's vitelliform dystrophy: Observation versus photodynamic therapy. *J Pediatr Ophthalmol Strabismus* 2010;47:121–2. [\[CrossRef\]](#)
- Andrade RE, Farah ME, Costa RA. Photodynamic therapy with verteporfin for subfoveal choroidal neovascularization in best disease. *Am J Ophthalmol* 2003;136:1179–81. [\[CrossRef\]](#)
- Leu J, Schrage NF, Degenring RF. Choroidal neovascularisation secondary to Best's disease in a 13-year-old boy treated by intravitreal bevacizumab. *Graefes Arch Clin Exp Ophthalmol* 2007;45:1723–5. [\[CrossRef\]](#)
- Khan KN, Mahroo OA, Islam F, Webster AR, Moore AT, Michaelides M. Functional and anatomical outcomes of choroidal neovascularization complicating BEST1-related retinopathy. *Retina* 2017;37:1360–70. [\[CrossRef\]](#)
- Schatz P, Bitner H, Sander B, Holfort S, Andreasson S, Larsen M, et al. Evaluation of macular structure and function by OCT and electrophysiology in patients with vitelliform macular dystrophy due to mutations in BEST1. *Invest Ophthalmol Vis Sci* 2010;51:4754–65. [\[CrossRef\]](#)
- Alisa-Victoria K, Jin-Poi T, Shatriah I, Zunaina E, Ngah NF. Choroidal neovascularization secondary to Best's vitelliform macular dystrophy in two siblings of a Malay family. *Clin Ophthalmol* 2014;12:537–42. [\[CrossRef\]](#)
- Marano F, Deutman AF, Leys A, Aandekerck AL. Hereditary retinal dystrophies and choroidal neovascularization. *Graefes Arch Clin Exp Ophthalmol* 2000;238:760–764. [\[CrossRef\]](#)
- Mandal S, Sinha S, Venkatesh P, Vashisht N. Intravitreal bevacizumab in choroidal neovascularization associated with Best's vitelliform dystrophy. *Indian J Ophthalmol* 2011;59:262–3.
- Cennamo G, Cesarano I, Vecchio EC, Reibaldi M, Crecchio G. Functional and anatomic changes in bilateral choroidal neovascularization associated with vitelliform macular dystrophy after intravitreal bevacizumab. *J Ocul Pharmacol Ther* 2012;28:643–6. [\[CrossRef\]](#)
- Chhablani J, Jalali S. Intravitreal bevacizumab for choroidal neovascularization secondary to Best vitelliform macular dystrophy in a 6-year-old child. *Eur J Ophthalmol* 2012;22:677–9. [\[CrossRef\]](#)
- Parodi MB, Zucchiatti I, Fasce F, Bandello F. Bilateral choroidal excavation in best vitelliform macular dystrophy. *Ophthalmic Surg Lasers Imaging Retina* 2014;14:45. [\[CrossRef\]](#)
- Parodi MB, Romano F, Arrigo A, Nunzio CD, Buzzotta A, Alto G. Natural course of the vitelliform stage in best vitelliform macular dystrophy: A five-year follow-up study. *Graefes Arch Clin Exp Ophthalmol* 2020;258:297–301. [\[CrossRef\]](#)